Synthesis, Electrochemistry, and Photophysics of Aza-BODIPY Porphyrin Dyes

Simon Pascal, Léo Bucher, Nicolas Desbois, Christophe Bucher, Chantal Andraud, Claude P. Gros

Synthesis, Electrochemistry and Photophysics of Aza-BODIPY Porphyrin Dyes

Simon Pascal,[a] Léo Bucher,[b] Nicolas Desbois,[b] Christophe Bucher,[a] Chantal Andraud,*[a] and Claude P. Gros,*[b]

[a] Dr S. Pascal, Dr. C. Bucher, Dr. C. Andraud
Laboratoire de Chimie, ENS Lyon-Université de Lyon1 (CNRS UMR 5182)
46 allée d'Italie, 69007 LYON, France
E-mail: chantal.andraud@ens-lyon.fr

[b] L. Bucher, Dr. N. Desbois, Prof. Dr. C. P. Gros
Institut de Chimie Moléculaire de l'Université de Bourgogne (ICMUB, UMR 6302)
9 Avenue Alain Savary, BP 47870, 21078 DIJON Cedex, France
E-mail: claude.gros@u-bourgogne.fr

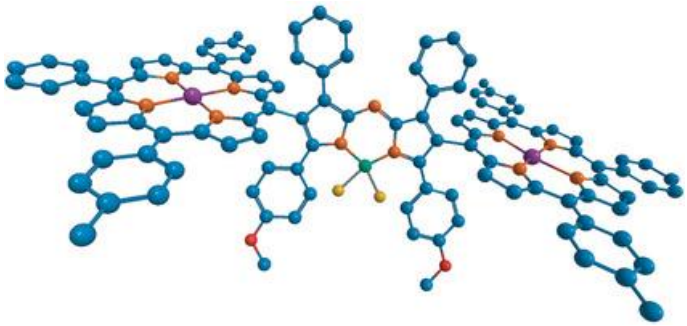

Abstract: The synthesis of two aza-BODIPY-porphyrin dyad and triad is described in two steps starting from a classical aza-BODIPY chromophore. These architectures have been extensively investigated in terms of optical and electrochemichal properties with a complete attribution of oxidation and reduction potentials using spectroelectrochemical methods. Fluorescence measurements revealed a dramatic loss of luminescence intensity mainly due to competitive energy transfer and photoinduced electron-transfer involving charge separation then recombination.

Introduction

BODIPYs (4,4-difluoro-4-bora-3a,4a-diaza-s-indacene) and porphyrins are versatile organic dyes that can easily be diversely functionalized to fine-tune their rich redox and optical properties (*e.g.* high extinction coefficient >80,000 $M^{-1}.cm^{-1}$ and high fluorescence quantum yield). When substituents yielding additional conjugation are added to the parent molecules, both the absorption and emission spectra of the resulting derivatives can shift to significantly longer wavelengths, with emission maxima greater than 750 nm.[1] Red, green, blue BODIPY derivatives that covered the full range of the visible spectrum have been reported in the literature,[1-2] as well as fluorescent conjugates of a variety of antibodies, peptides, proteins, tracers, and amplification substrates optimized for cellular labeling, imaging and detection.[1, 2b, 3] By analogy, aza-BODIPYs have been widely developed due to their significant red-shifted optical properties comparing to their parent *C*-BODIPYs, making them appropriate dyes for bio-imaging,[3b, 4] singlet oxygen generation[5], energy transfers[2l, 6] or nonlinear optics in the near-infrared range.[7]

Different BODIPY-porphyrin dyads have been also reported as functional models of the photosynthetic center, the BODIPY unit usually acting as the donor and the porphyrin macrocycle as the acceptor.[8] Recently, two examples of efficient singlet-singlet energy transfer in the opposite direction (*e.g.* from a zinc porphyrin) to a blue-BODIPY or an aza-BODIPY have been reported.[2p, 6b] Fluorescence Resonance Energy Transfers (RET) and Photoinduced Electron Transfers (PET) have been observed depending upon the nature of the spacer connected between the two fluorophores.

We report herein the synthesis of covalently linked aza-BODIPY-porphyrin tweezers linked at the β-position, which structures are shown in Chart 1. We were interesting to investigate their redox and photophysical properties, the aza-BODIPY being initially expected to work as an energy acceptor in the present polyads.

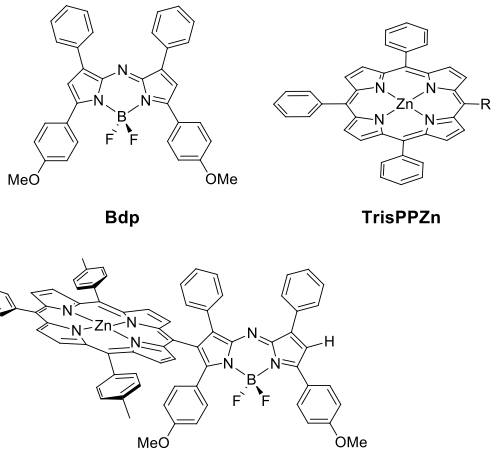

Chart 1

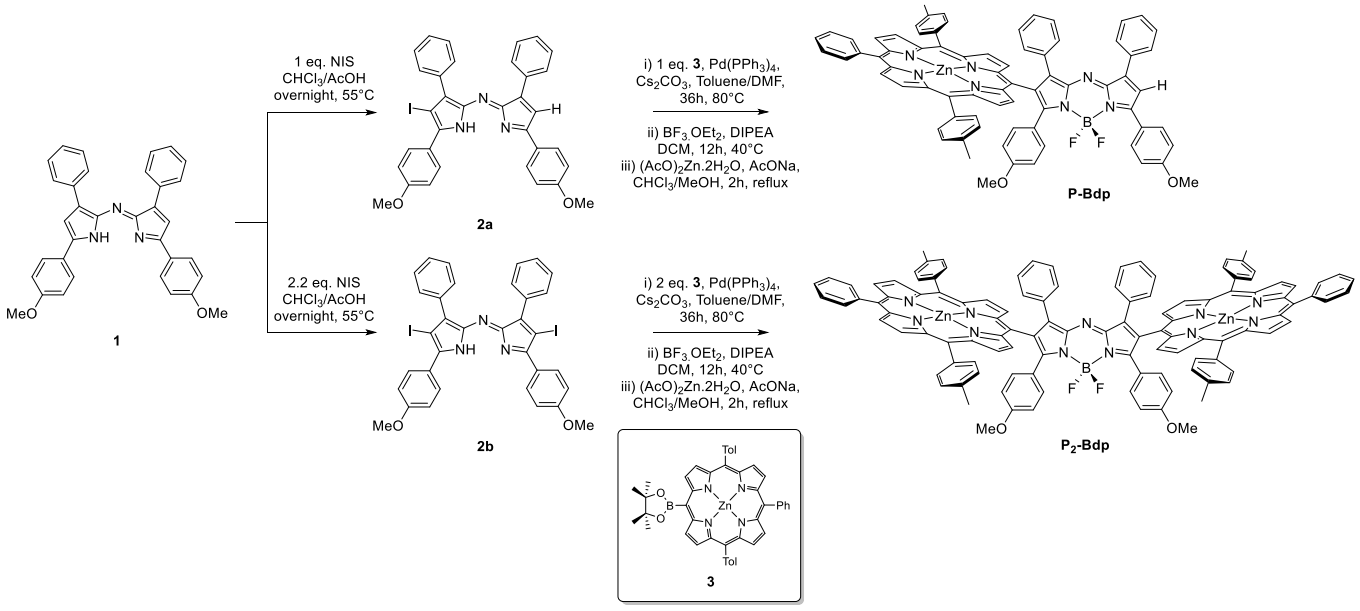

Scheme 1. Synthetic routes to dyad **P-Bdp** and triad **P_2-Bdp**. DCM = dichloromethane; DIPEA = *N*,*N*-diisopropylethylamine.

Results and Discussion

Synthesis

Mono and di-iodo aza-BODIPYs **2a-b** were both obtained by oxidation in presence of *N*-iodosuccinimide (NIS), according to protocols reported for the preparation of halogeno-BODIPYs used for photodynamic therapy applications.[5b, 5c] It is interesting to note that the introduction of one or two equivalents of NIS could respectively lead to the formation of either the mono- (**2a**) or the di-iodo (**2b**) aza-BODIPY derivatives. The Suzuki–Miyaura coupling reaction[9] between **2a** or **2b** and **3** is depicted in Scheme 1. Zinc-metallated porphyrin has been chosen because of its easiest purification, compared to its free base equivalent, and also because of the stability of the formed complex, which one could possibly prevent from unwelcome coordination between the porphyrin ring and other metal ions present during further reaction step. Tetrakis(triphenylphosphine)palladium(0) was introduced as catalyst in a toluene/DMF mixture, using cesium carbonate as a base in order to perform the coupling reaction between boronated porphyrin **3** and iodinated aza-BODIPY **2a** or **2b**. Once the synthons were coupled, the BODIPY fragments were directly chelated to boron under classical reaction conditions.

Compounds **P-Bdp** and **P_2-Bdp** were respectively isolated in 17 and 5 % yield and fully characterized by $^{1}H/^{13}C$ NMR, UV/Vis spectroscopy, and MALDI/TOF HRMS (Supporting Information, Figures S4-S7). HRMS measurements were performed using an MALDI/TOF instrument to further confirm the successful formation of compounds **P-Bdp** and **P_2-Bdp**. For instance, in the case of compound **P_2-Bdp**, the molecular peak is observed at *m/z* = 1809.5064 $[M]^{+\cdot}$ in the MALDI/TOF spectra (1809.5093 calcd for $C_{114}H_{78}BF_2N_{11}O_2Zn_2$), whereas for the mono-porphyrin derivative **P-Bdp**, the molecular peak is observed at *m/z* = 1183.3578 $[M]^{+\cdot}$ (1183.3541 calcd for $C_{74}H_{52}BF_2N_7O_2Zn$).

Electronic absorption

The chromophore **Bdp** exhibits a sharp absorption band centered at 692 nm characterized by a full width at half maximum ($\omega_{1/2}$) of 1170 cm^{-1} (Figure 1).

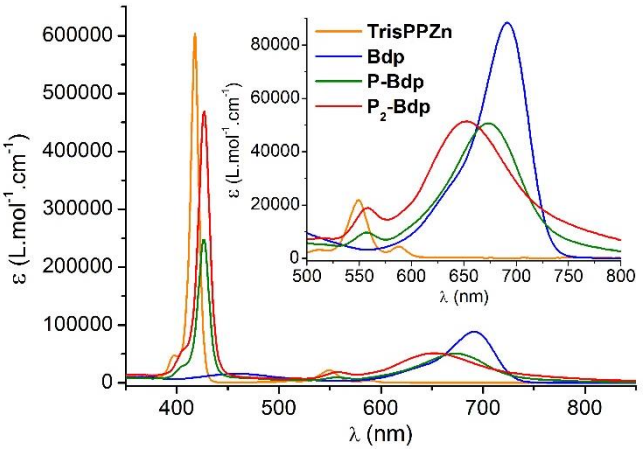

Figure 1. Absorption spectra of compounds **TrisPPZn**, **Bdp**, **P-Bdp** and **P_2-Bdp** in THF. Insert: absorption spectra in the visible range.

Table 1. Anodic and cathodic peak potentials (E_{pa}, E_{pc}) and half-wave potentials ($E_{1/2}$) values (mV) measured by CV for TrisPPZn, Bdp, P-Bdp and P_2-Bdp in DCM (TBAP 0.1 M) at a vitreous carbon electrode (Ø = 3 mm, v = 0.1 $V.s^{-1}$), *E* vs Ag/Ag^+. Red_n and Ox_n represent the n successive reduction and oxidation processes, respectively.

	Red_2			Red_1			Ox_1			Ox_2			Ox_3	Ox_4
	E_{pa}	E_{pc}	$E_{1/2}$	E_{pa}	E_{pc}	$E_{1/2}$	E_{pa}	E_{pc}	$E_{1/2}$	E_{pa}	Ep_c	$E_{1/2}$	E_{pa}	E_{pa}
TrisPPZn				-1608	-1673	-1640	507	453	480	856	798	827		
Bdp	-1444	-1509	-1476	-674	-741	-707	813	745	779	1030				1160
P-Bdp	-1380	-1520	-1450	-692	-758	-725	528	450	489	804			1040	1230
P_2-Bdp		-1548		-705	-775	-740	547	485	516	842	733	787		

Estimated experimental error = ± 5 mV; *E* ½ (Fc/Fc^+) = +200 mV *vs*. Ag/Ag^+

Macrocycle **TrisPPZn** displays classical porphyrins characteristics with an intense and sharp Soret transition localized at 420 nm and two Q bands with maxima around 550 and 590 nm. Absorption bands of **P-Bdp** and **P_2-Bdp** could be attributed on this basis. In the Soret region, **P_2-Bdp** possesses an absorption band with a two-fold intensity compared to that of **P-Bdp**, as a result of its second porphyrin fragment. A noticeable broadening of the aza-BODIPY transition is observed for **P-Bdp** and **P_2-Bdp** lower energy bands ($\omega_{1/2}$ of 1.800 and 2.300 cm^{-1} respectively), compared to that of **Bdp**, presumably due to a charge transfer from the electro-donating porphyrin extremity(ies) towards the strong electro-acceptor aza-BODIPY core; the broadening of absorption bands of aza-BODIPY moieties has been already shown to strongly depend on the nature of substituents and then on the strength of the charge transfer.[10] However, this charge transfer seems to be weak, due to the minor shift of the **P-Bdp** and **P_2-Bdp** absorption bands in the red region compared to that of **Bdp** and to the negligible solvatochromism observed for absorption and emission bands (Figures S8-S9).

Electrochemistry

The CV curves recorded for **Bdp** in an electrolytic DCM medium exhibits two Nernstian one-electron reduction waves (see (d) and (e) in Figure 2) attributed to the successive formation of **$Bdp^{\bullet-}$** and **Bdp^{2-}** at the electrode interface. The shift of about 0.77 V found between both reductions happens to be similar to that reported for the parent phenyl-substituted aza-BODIPY,[11] but much smaller than those usually found for carbon linked analogs. In the anodic domain, the voltammogram recorded in a stationary regime at a rotating disk electrode (doted curve in Figure 2) reveals the existence of two one-electron oxidation processes yielding **$Bdp^{\bullet+}$** and **Bdp^{2+}**. The observation of three successive waves on the CV curve (see (a), (b) and (c) in Figure 2) thus suggests the existence of an ECE type of mechanism, *i.e.* involving a chemical step most probably coupled to the first electron transfer (**$Bdp^{\bullet+} \rightarrow X$**, Figure 2).

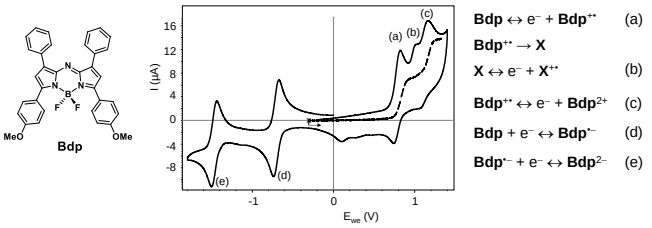

Figure 2. Voltammetric curves of a DCM (TBAP 0.1 M) solution of **Bdp** ($5 \cdot 10^{-4}$ M) recorded at (solid line) a vitreous working electrode (Ø = 3 mm, *E vs* Ag/Ag^+ (10^{-2} M), v = 0.1 $V.s^{-1}$) and (doted line) at a rotating vitreous carbon disk electrode (Ø = 3 mm, v = 0.01 $V.s^{-1}$, 500 rd/min).

This assumption is further supported by CV measurements carried out at different scan rates showing that the intensity of the second oxidation wave (wave (b) in Figure 3) goes down as the time scale of the measurement gets shorter. Recording the CV curve at 10 V/s led accordingly to the disappearance of wave (b) and to the observation of only two successive Nernstian oxidation processes ((a) and (c) in Figure 3). The instability of the oxidized forms of **Bdp** can reasonably be attributed to the absence of substitution at position 6 of the aza-BODIPY skeleton which does not prevent sigma dimerization to occur.

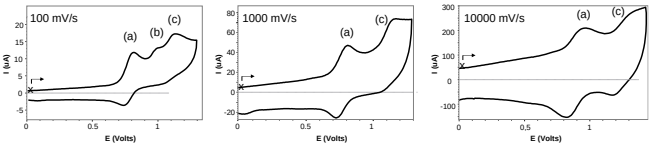

Figure 3. Voltammetric curves of a DCM (TBAP 0.1 M) solution of Bdp ($5 \cdot 10^{-4}$ M) recorded at a vitreous carbon electrode at v = 0.1, 1 and 10 $V.s^{-1}$ (Ø = 3 mm, *E vs* Ag/Ag^+ (10^{-2} M).

Electrochemical studies of the porphyrin-BODIPY derivative **P-Bdp** reveals the presence of three reduction and four oxidation waves (Figure 4A). The attribution of most processes seen on this CV curve could be achieved using the electrochemical signatures of **Bdp** and **TrisPPZn** as references (Figure 4C and Figure 4D). A key finding is that the "communication" between the porphyrin donor and the aza-BODIPY acceptor is quite weak, as revealed by the fact that the oxidation and reduction peak potentials measured on the voltammogram of **P-Bdp** almost fully match those corresponding to the isolated references **Bdp** and **TrisPPZn** (Figure 4).

A simple analysis of the data collected in Figure 4 especially reveals that the potential values corresponding to the first and second BODIPY-centered reductions as well as that of the first porphyrin-centered oxidation of **P-Bdp** (Figure 4A) fully match those measured on the CV curves of the reference compounds **Bdp** (Figure 4C) and **TrisPPZn** (Figure 4D), respectively. Based on these findings, the irreversible wave seen at E_{pa} = -1.9 V in the CV curve of **P-Bdp** (wave (g) in Figure 4A) can be unambiguously attributed to the first porphyrin-centered reduction which happens to be negatively shifted as compared to the reduction of the porphyrin reference **TrisPPZn.**

In the anodic domain, only the first wave seen at E_{pa} = 528 mV (Table 1) could be unambiguously attributed to the one-electron oxidation of the porphyrin donor in **P-Bdp** (wave (a) in Figure 4A). Ascribing the three following oxidation waves turned out to be made more difficult by the overlap of the reference oxidation potentials measured for **TrisPPZn** and **Bdp**.

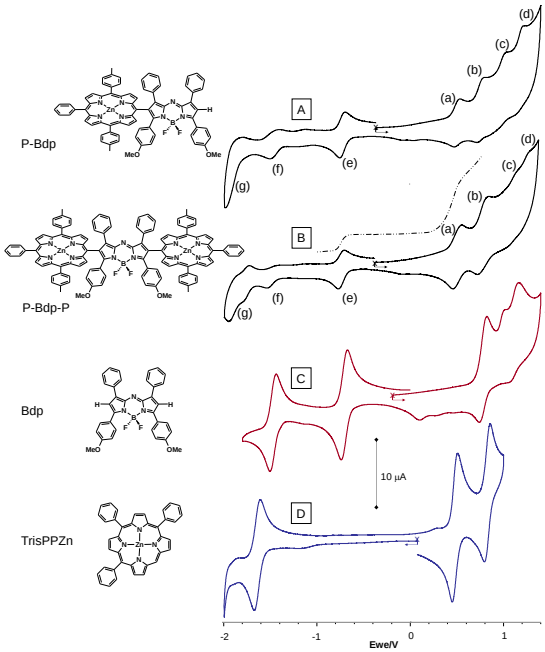

Figure 4. Voltammetric curves of DCM (TBAP 0.1 M) solutions of P-Bdp, P-Bdp-P, Bdp and trisPPZn ($5 \cdot 10^{-4}$ M) recorded (solid lines) at a vitreous carbon working electrode (Ø = 3 mm, *E vs* Ag/Ag^+ (10^{-2} M), v = 0.1 $V.s^{-1}$) and (dotted line) at a rotating carbon disk electrode (Ø = 3 mm, v = 0.01 $V.s^{-1}$, 500 rd/min).

Some insights into the attribution of these electron transfers could nevertheless be obtained upon carrying out "thin layer" spectroelectrochemistry (SEC) experiments. These analyses, conducted in a 0.5 mm SEC cell, consisted in recording periodically absorption spectra for solutions of P-Bdp submitted to a linear potential scan (20mV/s). In agreement with our assignment of waves (e) and (f) to the first and second reduction of the aza-BODIPY unit, scanning the working electrode potential from 0 to -1 V (Figure 5A) or from 0 to -1.7 V (Figure 5B) led to changes involving mainly the aza-BODIPY transition centred at ~680 nm. A two electron reduction of the aza-BODIPY unit even led to a complete disappearance of this broad signal at the expense of a less intense and red-shifted signal centered at ~800 nm (Figure 5B). Scanning the electrode potential from 0 to 0.55 V was conversely found to affect only the Soret band (Figure 5C), which is consistent with the formation of the porphyrin cation radical $P^{+\bullet}$-Bdp. The spectroelectrochemistry data shown in Figure 5 proved particularly useful in providing experimental support for the assignment of the three successive oxidation waves observed above 0.6 V (waves (b) (c) and (d) in Figure 4). We found for instance that the changes observed in the UV-Vis absorption spectra, as the working electrode potential is scanned up to the second oxidation wave, *i.e.* from 0 to 0.8 V, are compatible with an electron transfer centered on the aza-BODIPY unit to produce $P^{+\bullet}$-$Bdp^{+\bullet}$. This assumption is mainly supported by the fact that the broad transition at 676 nm undergoes a red-shift of about 10 nm while the intensity of the Soret band keeps going down. Further investigations, involving an extension of the potential scan up to 1 V, led us to conclude that the third oxidation wave observed at E_{pa3} ~ 1 V ((c) in Figure 5 involves the formation of the porphyrin dication, *i.e* $P^{+\bullet}$-$Bdp^{+\bullet} \rightarrow P^{2+}$-$Bdp^{+\bullet}$, this assumption being mostly based on the large drop in the intensity of the Soret band observed upon scanning. The fourth and last oxidation wave at 1.2 V was similarly attributed to the second oxidation of the aza-BODIPY unit, as suggested by the data shown in Figure 5F showing that scanning up to 1.2 V mainly impacts the broad band at ~700 nm.

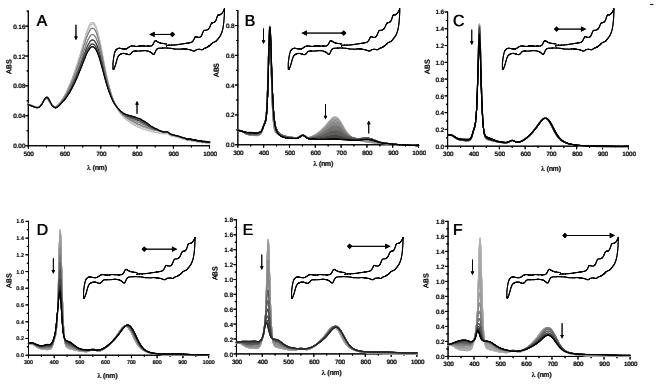

Figure 5. UV-vis-NIR spectral changes for solutions of **P-BdP** during (A) first reduction (B) second reduction (C) first oxidation, (D) second oxidation, (E) third oxidation, (F) fourth oxidation in DCM, 0.1 M TBAP.

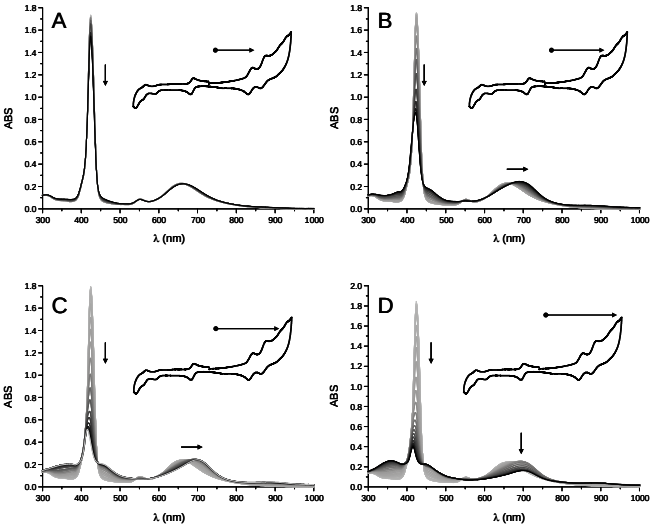

Figure 6. UV-vis spectral changes for solutions of **P_2-BdP** during (A) first oxidation, (B) second oxidation, (C) third oxidation, (D) fourth oxidation in DCM, 0.1 M TBAP.

The CV curves of the porphyrin-BODIPY derivative P_2-Bdp in DCM are shown in Figure 4FigureB together with those of the reference compounds TrisPPZn and Bdp. Here again, attributing the first oxidation ((a) in Figure 4B) and the two first reductions (d) and (e) Figure 4B) proved quite straightforward as the associated potential values fully match those measured on the CVs of the reference compounds TrisPPZn and Bdp. The relative number of electrons involved in the first oxidation (2 e/mol for wave (a)) and in the first reduction processes (1 e/mol for wave (e); see the slash-dotted line shown in Figure 4B) also reveal that both chemically equivalent porphyrin rings get oxidized at the same potential value E_{pa} ~ 0.5 V. On the cathodic side, the one-electron reduction waves, noted (e) and (f) in Figure 4, are then ascribed to the successive formation of $P\text{-}Bdp^{\bullet-}$-P and $P\text{-}Bdp^{2-}$-P, followed by two porphyrin-based one-electron reduction waves observed below -1.7 V (waves (g) in Figure 6B).

These attributions rely on comparisons with the CVs of the reference molecules supported by spectroelectrochemistry data. In agreement with the accumulation of $P^{+\bullet}$-Bdp-P and P^{+}-Bdp-$P^{+\bullet}$ in the SEC cell, the data shown in Figure 6A show for instance that the Soret band is the only signal being impacted when submitting the sample to a linear potential scan from 0 to 0.5 V. Extending the potential scan up to 0.9 V led conversely to changes affecting simultaneously the Soret and aza-BODIPY centered absorptions (Figure 6B), which suggest that the second two-electron oxidation wave (wave (b) in Figure 4B) involves an oxidation of the BODIPY unit. Further oxidations at 1.2 V or 1.4 V were similarly found to affect the porphyrin- and BODIPY-centered transitions, respectively.

One key conclusion drawn from these experimental evidences is that the second two-electron oxidation process (wave (b) on Figure 4B) most probably involves a one-electron oxidation of a porphyrin ring as well as a one electron oxidation of the aza-BODIPY unit, which implies that both porphyrin rings become electrochemically nonequivalent in the doubly oxidized species.

Steady-state luminescence and lifetime

The emission, luminescence lifetime and quantum yield were recorded in THF solution for dyad **P-Bdp**, triad **P_2-Bdp**, and their references fragments **TrisPPZn** and **Bdp**. The data are summarized in Table 2.

Table 2. Spectroscopic data in THF.

Compound	λ_{max} / nm (ε_{max} / 10^3.L.mol^{-1}.cm^{-1})	λ_{em} / nm[a]	τ / ns[c]	Φ [a][e]
Bdp	692 (88), 459 (16)	722[b]	2.6[d]	0.26[b]
TrisPPZn	588 (4), 549 (22), 418 (610)	648	2.2	0.026
		597	2.2	
P-Bdp	673 (51), 557 (10), 427 (247)	721	2.3	0.005
		657	2.0	
		609	2.0	
P_2-Bdp	653 (51), 558 (19), 427 (469)	721	2.4	<0.001
		657	1.8	
		609	2.0	

[a] Excitation at 550 nm. [b] Excitation at 650 nm. [c] NanoLED excitation at 573 nm. [d] NanoLED excitation at 655 nm. [c] Fluorescence quantum yield determined with total integration of the porphyrin and aza-BODIPY emission bands (error = ± 10%). Reference: Cresyl Violet (Φ = 0.55 in methanol).

The **Bdp** dye shows a strong luminescence in the near-infrared region depicted in Figure 7A, characterized by a good quantum yield (26%), with a lifetime of 2.6 ns and a particularly low Stokes shift (600 cm^{-1}). These data are consistent with the optical properties of this compound previously reported in chloroform solution.[12] Porphyrin reference **TrisPPZn** shows comparable emission spectrum with two maxima located at 600 and 650 nm, and a weak fluorescence quantum yield along with lifetime value of 2.2 ns (Figure 7A and Table 2).

The strong spectral overlap between emission spectrum of **TrisPPZn** with the absorption of **Bdp** allowed us to expect a resonant energy transfer (RET) process from the porphyrin to the aza-BODIPY in **P-Bdp** and **P_2-Bdp**. This assumption has been studied in the following.

The fluorescence of the polyads was measured when exciting at 550 nm, in the first Q transition. Both compounds **P-Bdp** and **P_2-Bdp** exhibit the structured emission bands at 609 and 657 nm from the porphyrin by comparison with Figure 7A, and a more intense band at lower energy (721 nm), attributed to the aza-BODIPY-centered fluorescence (Figure 7B-C). Fluorescence quantum yields of the porphyrin moieties are significantly weaker in polyads than in the corresponding reference compounds (0.005 and less than 0.001 for the total luminescence in **P-Bdp** and **P_2-Bdp** respectively, against 0.02 for **TrisPPZn,** as displayed in Table 2). This trend suggests a quenching through an energy and/or an electron transfer. The possibility of both phenomena will be evidenced thereafter.

It is worth noting that the porphyrin emission increases with respect to that of the aza-BODIPY part in **P_2-Bdp** (Figure 7C); this trend will be subsequently discussed. The observation of the emission from the aza-BODIPY core, when exciting mainly in porphyrins bands at 550 nm, could have two origins: (1) an energy transfer between both moieties after excitation of the porphyrin, (2) a simultaneous excitation in the tail of absorption bands of the aza-BODIPY core and in the Q band of the porphyrin. The significant decrease of the total emission quantum yield (including the Q band and the emission of the aza-BODIPY core) observed under the 550 nm excitation in **P_2-Bdp** (0.005 versus less than 0.001 for **P-Bdp** and **P_2-Bdp** respectively), in spite of a higher absorption coefficient at this wavelength (Figure 7C and Table 2), could arise from the existence of a RET phenomenon or from its enhancement in **P_2-Bdp**. The excitation spectra of the 750 nm emission of polyads **P-Bdp** and **P_2-Bdp** in THF contain the bands of the **Bdp** reference at 460 and 660 nm, with no contribution of the Q bands from the porphyrin(s) fragment(s) (Figure 7B and C); however the observation of the Soret band for both compounds around 400 nm is a clear proof of a RET within **P-Bdp** and **P_2-Bdp.** This RET process seems to be higher in **P_2-Bdp**, which exhibits a Soret excitation band as intense as the highest energy excitation band of the aza-BODIPY core around 450 nm; however, the weak intensity of this Soret excitation band, which is the most intense in absorption spectra of these polyads, with respect to those of the aza-BODIPY, is the sign of the low efficiency of the RET process. This could explain the lack of the Q bands, which present lower absorption coefficients, in the excitation spectra of the aza-BODIPY-centered emission.

A similar study has been performed in toluene and DCM instead of THF. As well as we observed in THF, the RET seems to be more efficient in **P_2-Bdp,** which shows a higher Soret excitation band for emission at 720 nm (more intense or slightly less intense than the 460 nm excitation band in toluene and DCM respectively, as displayed in Figures S10 and S11 respectively). The main difference with observations in THF are the relative emissions intensities of the porphyrin and the aza-BODIPY parts under 550 nm excitation: the last one dominates in **P-Bdp** for the three solvents, whereas in **P_2-Bdp** the former is more intense in toluene and DCM (Figure S9). This trend will be discussed in the following. However, in the three solvents, the Soret band keeps overall a similar intensity compared to those of the aza-BODIPY bands in the excitation spectra of polyads, which suggests that the strength of the RET process does not seem to depend on the solvent.

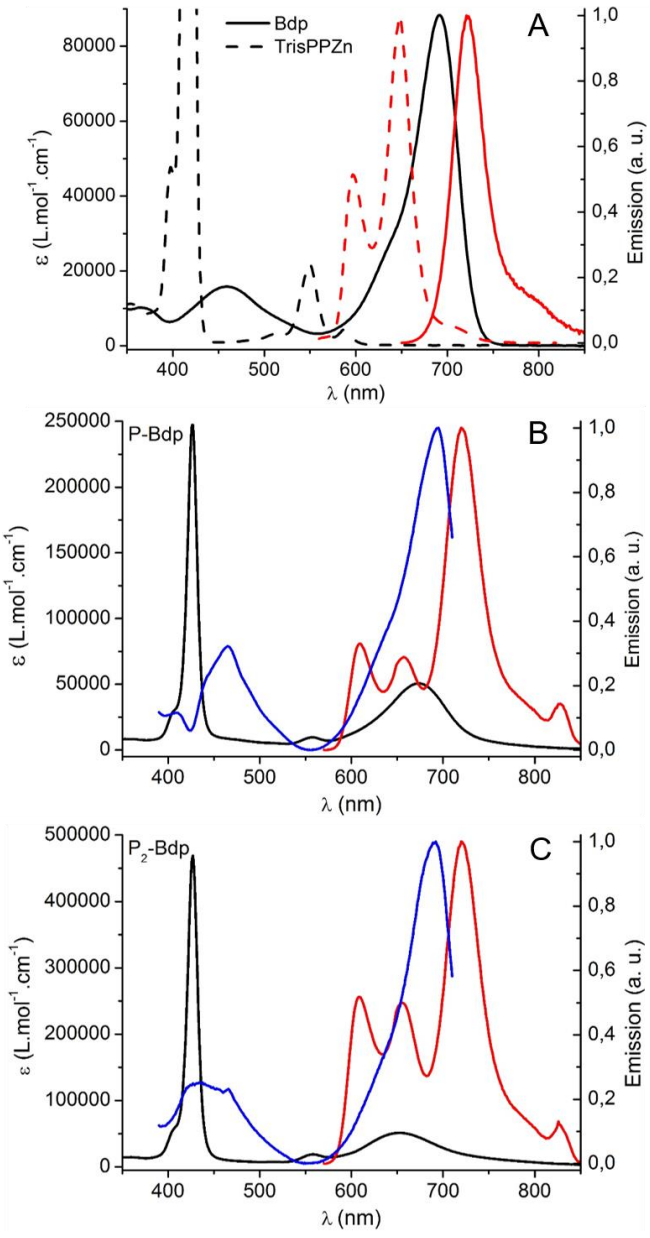

Figure 7. Absorption (black), emission (red) spectra of compounds (A) **Bdp**, and **TrisPPZn**, (B) **P-Bdp** and (C) **P_2-Bdp** in THF; excitation spectra (blue) of 750 nm emission of (B) **P-Bdp** and (C) **P_2-Bdp** in THF.

It is worth noting that the fluorescence lifetimes of porphyrin emission bands are slightly shorter in polyads in good agreement with the existence of the energy transfer from porphyrins to the aza-BODIPY moiety (Tables S1 and S2).

However, the weakness of this energy transfer led us to consider the existence of a competitive photoinduced electron transfer (PET) process.[8] This PET hypothesis within the polyads was investigated by determining the free enthalpy relative to charge separation (ΔG_{CS}), using the simplified Rehm-Weller equation:[13]

$$\Delta G_{CS} = (E_{ox} - E_{red}) - E_s \quad \text{Eq (1)}$$

where E_{ox} and E_{red} are the measured oxidation and redox potentials respectively and E_s corresponds to the excited state energy deduced from the zero-phonon transition. According to experimental data, the porphyrin fragments of **P-Bdp** and **P$_2$-Bdp** are respectively oxidized at 0.489 and 0.516 eV, and their aza-BODIPY centers are reduced at -0.725 and -0.740 eV. The excited state energies were determined to be 1.761 and 1.763 eV in DCM, leading to charge separation free enthalpy equal to -0.547 and -0.507 eV, respectively for **P-Bdp** and **P$_2$-Bdp**. Since negative values are obtained for ΔG_{CS}, the dissipation of the energy *via* a charge separation and recombination is therefore thermodynamically favored in DCM solution.

The evolution of the PET phenomenon has been also investigated within both polyads and as a function of the solvent, through the relative emission intensities of the porphyrins and of the aza-BODIPY when exciting at 550 nm (Figure S9). In the three solvents, in **P-Bdp**, in which a weak RET has been shown previously, the emission of the porphyrin is significantly weaker than that of the aza-BODIPY (Figure S9), due to the PET. This trend increases from the THF to toluene and DCM, which corresponds to the variations of the solvents polarity; in polar solvents the energy E_s, in the relationship (1), is expected to decrease, leading to an increase of the PET.

Moreover, in **P$_2$-Bdp** the porphyrin emission becomes the most intense in DCM and toluene, suggesting a drop of the PET strength in **P$_2$-Bdp** in favor of the RET process; this trend is in good agreement with the relative ΔG_{CS} values in **P-Bdp** and **P$_2$-Bdp,** as pointed out above**.** Although this trend is less significant in THF, since the aza-BODIPY emission remains the most important in **P$_2$-Bdp**, the enhancement of the porphyrin emission can be interpreted in a same way.

Conclusion

Examples of a new class of mono- and di-porphyrin aza-BODIPY conjugates featuring direct covalent linkage between a porphyrin ring and a BODIPY unit have been prepared. The properties of these novel polyads have been comprehensively investigated by means of absorption/emission spectroscopy, electrochemistry, and spectroelectrochemistry. The electrochemical signatures of the dyad and triad have been fully interpreted on the basis of CV and spectroelectrochemical data. Absorption and electrochemical measurements revealed weak charge transfer and limited "communication" between the porphyrin donor and the aza-BODIPY acceptor fragments. However, energy transfer from the porphyrin to the aza-BODIPY center has been shown to occur, with competitive photoinduced electron transfer, in good agreement with the spectroelectrochemical properties of **P-Bdp** and **P$_2$-Bdp**.

Experimental Section

Instrumentation

The NMR spectra were recorded at room temperature on a Bruker Avance spectrometer operating at 500 MHz for ^{1}H, 125 MHz for ^{13}C and 188 MHz for ^{19}F, at the ENS Lyon; and on a Bruker Avance Bruker Avance II 300 spectrometer operating at 300 MHz for ^{1}H, 75 MHz for ^{13}C, 96 MHz for ^{11}B and 282 MHz for ^{19}F at the *Welience, Pôle Chimie Moléculaire de l'Université de Bourgogne* (*WPCM*). Chemical shifts (δ) are listed in parts per million (ppm) relative to residual solvent peaks being used as internal standard (^{1}H ($CDCl_3$): 7.26 ppm, ^{13}C ($CDCl_3$): 77.2 ppm; ^{1}H (CD_2Cl_2): 5.32 ppm, ^{13}C (CD_2Cl_2): 53.8 ppm). UV–visible spectra were recorded on a Jasco V-670 spectrophotometer in spectrophotometric grade THF, DCM or toluene solutions (*c.a.* 10^{-6} mol.L^{-1}). Molar extinction coefficients (ε) were determined two times in THF or DCM. Mass spectra and accurate mass measurements (HRMS) were obtained on a Bruker Daltonics Ultraflex II spectrometer in the MALDI/TOF reflectron mode using dithranol as a matrix or on a LTQ Orbitrap XL (THERMO) instrument in ESI mode. Both measurements were registered at *WPCM*.

Luminescence

The luminescence spectra were measured using a Horiba-Jobin Yvon Fluorolog-3 iHR320 spectrofluorimeter, equipped with a three slit double grating excitation and emission monochromator with dispersions of 2.1 nm/mm (1200 grooves/mm). The steady-state luminescence was excited by unpolarized light from a 450W xenon CW lamp and detected at an angle of 90° for diluted solutions in 10 mm quartz cuvette by a near infrared-sensitive R2658 PMT photomultiplier tube. Spectra were reference corrected for both the excitation source light intensity variation (lamp and grating) and the emission spectral response (detector and grating). Fluorescence quantum yields Φ were measured in diluted THF solutions with an optical density lower than 0.1 and determined using the following equation $\Phi_x/\Phi_r = [A_r(\lambda)/A_x(\lambda)][n_x^2/n_r^2][D_x/D_r]$ were A is the absorbance at the excitation wavelength (λ), n the refractive index and D the integrated intensity. "r" and "x" stand for reference and sample. Here the reference is Cresyl Violet (Φ = 0.55 in methanol). Excitation of reference and sample were performed at the same wavelength. Short luminescence decay was monitored with the TC-SPC Horiba apparatus using Ludox in distilled water to determine the instrumental response function used for deconvolution. Excitation was performed using NanoLEDs, with models (peak wavelength; pulse duration) 440 (440 nm; <250 ps), 570 (573 nm; 1.5 ns), and 650 (655 nm; <200 ps). The deconvolution was performed using the DAS6 fluorescence-decay analysis software.

Electrochemistry and spectroelectrochemistry

Cyclic voltammetry (CV) data have been recorded using an ESP-300 Biologic potentiostat equipped with a 1 A/48 V booster and an analog linear scan generator. All the experiments were conducted under an argon atmosphere in a standard one-compartment, three-electrode electrochemical cell placed in a faraday cage. Tetra-*n*-butylammonium perchlorate (TBAP) in anhydrous DCM was used as supporting electrolytes (0.1 M). An automatic ohmic drop compensation procedure was systematically implemented prior to recording CV data. All the electrodes were purchased from ALS Co. Ltd. Vitreous carbon (Ø = 3 mm) working electrodes were polished with 1 mm diamond paste before each recording. An $Ag|AgNO_3$ (10^{-2} M + TBAP 10^{-1} M in CH_3CN) electrode was used as a reference. Spectroelectrochemical measurements have been carried out with a Biologic ESP-300 potentiostat coupled to an MCS 500 UV-NIR Zeiss spectrophotometer using either "thin layer" (0.5 mm or 1 mm) SEC cells purchased from ALS Co. Ltd. Voltamperometry experiments involving rotating disk electrodes (RDE) have been carried out with a Radiometer equipment at a rotation rate of 550 rd·min^{-1} using a glassy carbon RDE tip (Ø = 3 mm). A standard sweep rate of 0.01 V.s^{-1} was used in RDE experiments.

Materials

The starting material aza-BODIPY **1**,[12] the boronic ester porphyrin **3**[14] and the aza-dipyrromethene **2b**[15] were prepared according to literature procedures. Unless otherwise noted, all chemicals and solvents were of analytical reagent grade and used as received. Absolute dichloromethane (DCM) was obtained from Carlo Erba. Silica gel (Merck; 70-120 mm) was used for column chromatography. Analytical thin-layer chromatography was performed with Merck 60 F_{254} silica gel (precoated sheets, 0.2 mm thick). Reactions were monitored by thin-layer chromatography, UV/Vis spectroscopy and MALDI/TOF mass spectrometry.

2-iodo-1,9-di(4'-methoxyphenyl)-3,7-phenyl-aza-dipyrromethene (2a). 200 mg of **1** (0.39 mmol, 1 eq.) were dissolved in 20 mL of degassed $CHCl_3$ and acetic acid glacial (3:1). 88 mg of NIS (0.39 mmol, 1 eq.) was added and the reaction was stirred for 16 h at 55°C. The crude reaction mixture was diluted in 30 mL of DCM and washed with an aqueous saturated Na_2O_5S solution (50 mL), an aqueous saturated Na_2CO_3 solution (50 mL) and water (30 mL). The aqueous layers were extracted with DCM (2 x 10 mL) and the combined organic layers were dried over Na_2SO_4 and concentrated. The crude residue was purified by flash chromatography on silica gel with petroleum ether/DCM as eluent (1:1, R_f = 0.53). The product **2a** was obtained as a dark blue solid in 76 % yield (189 mg). ^{1}H NMR (CD_2Cl_2, 500 MHz): δ 8.11 (d, ^{3}J = 8 Hz, 2H, CH_{Ar}), 8.01 (d, ^{3}J = 7 Hz, 2H,

CH_{Ar}), 7.88 (d, ^3J = 8 Hz, 2H, CH_{Ar}), 7.76 (d, ^3J = 7 Hz, 2H, CH_{Ar}), 7.52 (t, ^3J = 7 Hz, 2H, CH_{Ar}), 7.45 (t, ^3J = 7 Hz, 1H, CH_{Ar}), 7.35-7.30 (m, 3H, CH_{Ar}), 7.22 (s, 1H, CH_{Ar}), 7.12 (d, ^3J = 8 Hz, 2H, CH_{Ar}), 7.05 (d, ^3J = 8 Hz, 2H, CH_{Ar}), 3.93 (s, 3H, OCH_3), 3.90 (s, 3H, OCH_3). ^{13}C NMR (CD_2Cl_2, 125 MHz): δ 162.4 (C_{quat}), 161.6 (C_{quat}), 156.5 (C_{quat}), 153.4 (C_{quat}), 150.2 (C_{quat}), 148.8 (C_{quat}), 145.5 (C_{quat}), 143.3 (C_{quat}), 134.4 (C_{quat}), 133.6 (C_{quat}), 131.3 (CH), 131.1 (C_{quat}), 130.9 (CH), 129.1 (CH), 129.3 (CH), 128.6 (CH), 128.6 (CH), 128.4 (CH), 128.0 (CH), 126.1 (C_{quat}), 124.5 (C_{quat}), 115.5 (N-C-CH), 115.1 (CH), 114.4 (CH), 55.9 (OCH_3), 55.9 (OCH_3). UV-Vis (CH_2Cl_2): λ_{max} = 605 nm (ε_{max} = 32 000 $L.mol^{-1}.cm^{-1}$). HRMS (ESI^+): $[M+H]^+$ = 636.1122 (calcd for $C_{34}H_{27}N_3O_2$: 636.1142).

2-(Porphyrin Zn(II)) aza-BODIPY (P-Bdp). 5,15-(*p*-Tolyl)-10-(phenyl)-20-(4',4',5',5'-tetramethyl-[1',2',3']dioxaboran-2'-yl) porphyrin Zinc(II) **3** (118 mg, 0.156 mmol), 2-iodo-1,9-di(4'-methoxyphenyl)-3,7-phenyl-aza-dipyrromethene **2a** (90 mg, 0.142 mmol), cesium carbonate (92 mg, 0.284 mmol) and *tetrakis*(triphenylphosphine)palladium(0) (8 mg, 0.007 mmol) were dissolved under argon in 55 mL of freshly distilled toluene and 40 mL of dry DMF. After stirring the mixture for 36 h at 80°C, the reaction solvent was removed by evaporation under reduced pressure. The crude residue was dissolved in 30 mL of DCM and washed with water (3x30 mL). The organic layer was dried over $MgSO_4$ and then evaporated. The compound was quickly purified by silica gel flash column chromatography using *n*-heptane/DCM (9:1) to pure DCM as eluting conditions. The product thus obtained was dissolved in 6 mL DCM and DIPEA (241 μL, 1.420 mmol). Boron trifluoride etherate (560 μL, 2.130 mmol) was added and the reaction mixture was heated at 40°C and stirred for 12 h. The crude mixture was washed with water (3x20 mL), dried over $MgSO_4$ and evaporated. The crude product was dissolved in a mixture of 9 mL $CHCl_3$/MeOH (2:1) to which were added zinc acetate dihydrate (312 mg, 1.420 mmol) and sodium acetate (232 mg, 2.840 mmol). This solution was refluxed overnight and finally evaporated. The residue was dissolved in 20 mL of DCM, washed with water (3x20 mL), dried over $MgSO_4$, concentrated and purified by silica preparative chromatography using *n*-heptane/DCM (4:6) as eluent to obtain compound **P-Bdp** as a blue-violet solid in 17 % yield (29 mg, 4.422 μmol). ^1H NMR ($CDCl_3$, 600 MHz): δ 9.16 (d, ^3J = 4.7 Hz, 2H, $H_{\beta\text{-pyrr porphyrin}}$), 8.90 (d, ^3J = 4.4 Hz, 2H, $H_{\beta\text{-pyrr porphyrin}}$), 2.69 (s, 6H, $CH_{3\ tolyl}$), 8.86 (d, ^3J = 4.4 Hz, 4H, $H_{\beta\text{-pyrr porphyrin}}$), 8.24 (d, ^3J = 7.8 Hz, 2H, $H_{m\text{-phenyl}}$), 8.21 (d, ^3J = 7.8 Hz, 1H, $H_{p\text{-phenyl}}$), 8.18 (d, ^3J = 9.0 Hz, 2H, $H_{o\text{- methoxyphenyl}}$), 8.15 (d, 1H, $H_{p\text{-phenyl}}$), 8.04 (d, ^3J = 7.8 Hz, 4H, $H_{o\text{-tolyl porphyrin}}$), 7.73 (m, 4H, $H_{o\text{-phenyl porphyrin}}$, $H_{m\text{-phenyl porphyrin}}$), 7.52 (dd, ^3J = 7.8 Hz, 4H, $H_{m\text{-tolyl porphyrin}}$), 7.45 (d, ^3J = 7.8 Hz, 2H, $H_{o\text{-phenyl}}$), 7.32 (d, ^3J = 7.8 Hz, 2H, $H_{o\text{-phenyl}}$), 7.31 (d, ^3J = 9.0 Hz, 2H, $H_{o\text{- methoxyphenyl}}$), 7.21 (s, 1H, $H_{\beta\text{-pyrr azaBODIPY}}$), 7.03 (d, ^3J = 9.0 Hz, 2H, $H_{m\text{-methoxyphenyl}}$), 6.78 (dd, ^3J = 7.8 Hz, 1H, $H_{p\text{-phenyl}}$), 6.60 (dd, ^3J = 7.8 Hz, 2H, $H_{m\text{-phenyl}}$), 5.99 (d, ^3J = 9.0 Hz, 2H, $H_{m\text{-methoxyphenyl}}$), 3.89 (s, 3H, $CH_{3\ methoxy}$),3.20 (s, 3H, $CH_{3\ methoxy}$). ^{13}C NMR ($CDCl_3$, 125 MHz): δ 165.6 (C_{quat}), 165.5 (C_{quat}), 162.4 (C_{quat}), 161.9 (C_{quat}), 159.9 (C_{quat}), 150.9 (C_{quat}), 150.6 (C_{quat}), 150.4 (C_{quat}), 150.1 (C_{quat}), 143.1 (C_{quat}), 139.9 (C_{quat}), 137.2 (C_{quat}), 134.6 (CH), 134.5 (CH), 134.3 (C_{quat}), 134.3 (CH), 134.3 (CH), 133.9 (C_{quat}), 133.1 (CH), 132.7 (C_{quat}), 132.5 (C_{quat}), 132.3 (C_{quat}), 132.0 (CH), 131.8 (CH), 131.1 (CH), 131.1 (CH), 130.5 (C_{quat}), 129.9 (CH), 129.5 (CH), 128.9 (CH), 128.8 (CH), 127.8 (CH), 127.6 (CH), 127.4 (CH), 126.6 (CH), 124.2 (C_{quat}), 121.1 (C_{quat}), 118.1 (CH), 114.6 (CH), 112.9 (CH), 110.5 (C_{quat}), 55.6 (OCH_3), 54.4 (OCH_3), 21.6 (CH_3). ^{11}B NMR ($CDCl_3$, 96 MHz): δ 1.36 (t, ^1J = 30.8 Hz). ^{19}F NMR ($CDCl_3$, 282 MHz): δ -131.43 (q, ^1J = 30.8 Hz). UV-Vis (THF): λ_{max} = 673 nm (ε_{max} = 50 600 $L.mol^{-1}.cm^{-1}$). HRMS (MALDI/TOF): $[M^+]$ = 1183.3578 (calcd for $C_{74}H_{52}BF_2N_7O_2Zn^+$: 1183.3541).

2,6-bis(Porphyrin Zn(II)) aza-BODIPY (P_2-Bdp). 5,15-(*p*-Tolyl)-10-(phenyl)-20-(4',4',5',5'-tetramethyl-[1',2',3']dioxaboran-2'-yl) porphyrin zinc(II) **3** (152 mg, 0.202 mmol), 2,8-diiodo-1,9-di(4'-methoxyphenyl)-3,7-phenyl aza-dipyrromethene **2b** (77 mg, 0.101 mmol), cesium carbonate (82 mg, 0.253 mmol) and tetrakis(triphenylphosphine)palladium(0) (12 mg, 0.01 mmol) were dissolved under argon in 60 mL of freshly distilled toluene and 45 mL of dry DMF. After 36 h at 80°C, the reaction solvent was removed by evaporation under reduced pressure. The crude product was dissolved in 30 mL of DCM and washed with water (3x30 mL). The organic layer was dried over $MgSO_4$ and then evaporated. The compound was quickly purified by silica gel column flash chromatography using *n*-heptane/DCM (9:1) to pure DCM as eluting conditions. The product thus obtained was dissolved in 5 mL DCM and DIPEA (172 μL, 1.010 mmol). Boron trifluoride etherate (401 μL, 1.520 mmol) was added and the reaction mixture was heated at 40 °C and stirred for 12 h. The crude reaction was washed with water (3x20 mL), dried over $MgSO_4$ and evaporated. The crude product was dissolved in a mixture of 7.5 mL $CHCl_3$/MeOH (2:1) to which were added zinc acetate dihydrate (222 mg, 1.010 mmol) and sodium acetate (170 mg, 2.021 mmol). This solution was refluxed overnight and finally evaporated. The residue was dissolved in 20 mL of DCM, washed with water (3x20 mL), dried over $MgSO_4$, evaporated and purified by silica preparative chromatography using *n*-heptane/DCM (4:6) as eluent to afford compound **P_2-Bdp** as a blue-violet solid in 5 % yield (8 mg, 4.422 μmol). ^1H NMR ($CDCl_3$, 500 MHz): δ 9.30 (d, ^3J = 4.8 Hz, 4H, $H_{\beta\text{-pyrr porphyrin}}$), 8.95 (d, ^3J = 4.8 Hz, 8H, $H_{\beta\text{-pyrr porphyrin}}$), 8.90 (d, ^3J = 4.8 Hz, 4H, $H_{\beta\text{-pyrr porphyrin}}$), 8.21 (d, ^3J = 7.8 Hz, 8H, $H_{o\text{-tolyl porphyrin}}$), 8.18 (d, ^3J = 8.5 Hz, 2H, $H_{p\text{-phenyl}}$), 7.75 (t, ^3J = 8.5 Hz, 4H, $H_{m\text{-phenyl}}$), 7.54 (d, ^3J = 8.5 Hz, 4H, $H_{o\text{-phenyl}}$), 7.51 (m, ^3J = 7.8 Hz, 8H, $H_{m\text{-tolyl porphyrin}}$), 7.45 (d, ^3J = 7.8 Hz, 4H, $H_{o\text{-phenyl}}$), 7.41 (d, ^3J = 9.2 Hz, 4$H_{o\text{-methoxyphenyl}}$), 6.78 (d, ^3J = 7.4 Hz, 2H, $H_{p\text{-phenyl}}$), 6.61 (dd, ^3J = 7.8 Hz, ^3J = 7.4 Hz, 4H, $H_{m\text{-phenyl}}$), 6.02 (d, ^3J = 9.2 Hz, 4H, $H_{m\text{-methoxyphenyl}}$), 3.20 (s, 6H, $CH_{3\ methoxy}$), 2.72 (s, 12H, $CH_{3\ tolyl}$). ^{13}C NMR ($CDCl_3$, 125 MHz): δ 160.5 (C_{quat}), 160.1 (C_{quat}), 150.9 (C_{quat}), 150.6 (C_{quat}), 150.4 (C_{quat}), 150.1 (C_{quat}), 143.5 (C_{quat}), 143.2 (C_{quat}), 140.0 (C_{quat}), 137.2 (C_{quat}), 134.7 (CH), 134.6 (CH), 134.5 (CH), 133.2 (CH), 132.6 (C_{quat}), 132.0 (CH), 131.8 (CH), 131.2 (CH), 131.1 (CH), 128.0 (CH), 127.6 (CH), 127.5 (CH), 127.4 (CH), 126.6 (CH), 124.1 (C_{quat}), 121.7 (C_{quat}), 121.1 (C_{quat}), 113.0 (CH), 110.3 (C_{quat}), 54.7 (OCH_3), 21.7 (CH_3). ^{11}B NMR ($CDCl_3$, 160 MHz): δ 1.64 (t, ^1J = 31.0 Hz). ^{19}F NMR ($CDCl_3$, 470 MHz): δ -130.27 (q, ^1J = 31.0 Hz). UV-Vis (THF): λ_{max} = 653 nm (ε_{max} = 51 300 $L.mol^{-1}.cm^{-1}$). HRMS (MALDI/TOF): $[M^+]$ = 1809.5064 (calcd for $C_{114}H_{78}BF_2N_{11}O_2Zn_2^+$: 1809.5093).

Acknowledgements

The "Centre National de la Recherche Scientifique" (ICMUB, UMR CNRS 6302) is gratefully thanked for financial support. Support was provided by the CNRS, the "Université de Bourgogne" and the "Conseil Régional de Bourgogne" through the 3MIM integrated project ("Marquage de Molécules par les Métaux pour l'Imagerie Médicale"). SP and LB thank the French Ministry of Research for PhD grants. Fanny Picquet and Marie José Penouilh are warmly acknowledged for technical support.

Keywords: Polyads • aza-BODIPY • porphyrin • fluorescence spectroscopy • spectroelectrochemistry • photoinduced electron transfer

References

[1] A. Loudet, K. Burgess, *Chem. Rev.* **2007**, *107*, 4891-4932.

[2] a) X. L. Zhang, Y. Xiao, X. H. Qian, *Org. Lett.* **2008**, *10*, 29-32; b) G. Ulrich, R. Ziessel, A. Harriman, *Angew. Chem. Int. Ed.* **2008**, *47*, 1184-1201; c) J.-Y. Liu, M. E. El-Khouly, S. Fukuzumi, D. K. P. Ng, *Chem. Asian J.* **2011**, *6*, 174-179; d) C. Y. Lee, J. T. Hupp, *Langmuir* **2010**, *26*, 3760-3765; e) M. Koepf, A. Trabolsi, M. Elhabiri, J. A. Wytko, D. Paul, A. M. Albrecht-Gary, J. Weiss, *Org. Lett.* **2005**, *7*, 1279-1282; f) Z. Y. Gu, D. S. Guo, M. Sun, Y. Liu, *J. Org. Chem.* **2010**, *75*, 3600-3607; g) Y. Gabe, Y. Urano, K. Kikuchi, H. Kojima, T. Nagano, *J. Am. Chem. Soc.* **2004**, *126*, 3357-3367; h) Z. Dost, S. Atilgan, E. U. Akkaya, *Tetrahedron* **2006**, *62*, 8484-8488; i) A. Coskun, E. U. Akkaya, *J. Am. Chem. Soc.* **2005**, *127*, 10464-10465; j) F. Camerel, G. Ulrich, J. Barbera, R. Ziessel, *Chem. Eur. J.* **2007**, *13*, 2189-2200; k) T. Bura, P. Retailleau, G. Ulrich, R. Ziessel, *J. Org. Chem.* **2011**, *76*, 1109–1117; l) G. Barin, M. D. Yilmaz, E. U. Akkaya, *Tetrahedron Lett.* **2009**, *50*, 1738–1740; m) E. U. Akkaya, O. A. Bozdemir, R. Guliyev, O. Buyukcakir, S. Selcuk, S. Kolemen, G. Gulseren, T. Nalbantoglu, H. Boyaci, *J. Am. Chem. Soc.* **2010**, *132*, 8029-8036; n) B. Brizet, A. Eggenspiller, C. P. Gros, J.-M. Barbe, C. Goze, F. Denat, P. D. Harvey, *J. Org. Chem.* **2012**, *77*, 3646-3650; o) B. Brizet, N. Desbois, A. Bonnot, A. Langlois, A. Dubois, J.-M. Barbe, C. P. Gros, C. Goze, F. Denat, P. D. Harvey, *Inorg. Chem.* **2014**, *53*, 3392-3403; p) A. Eggenspiller, A. Takai, M. E. El-Kouhly, K. Ohkubo, C. P. Gros, C. Bernhard, C. Goze, F. Denat, J.-M. Barbe, S. Fukuzumi, *J. Phys. Chem. A.* **2012**, *116*, 3889-3898; q) H.-J. Xu, A. Bonnot, P.-L. Karsenti, A. Langlois, M. Abdelhammed, J.-M. Barbe, C. P. Gros, P. D. Harvey, *Dalton Trans.* **2014**, *43*, 8219-8229; r) A. L. Nguyen, P. Bobadova-Parvanova, M. Hopfinger, F. R. Fronczek, K. M. Smith, M. G. H. Vicente, *Inorg. Chem.* **2015**, ASAP.

[3] a) N. Boens, V. Leena, W. Dehaen, *Chem. Soc. Rev.* **2012**, *41*, 1130-1172; b) A. Kamkaew, S. Hui Lim, H. Boon Lee, L. Voon Kiew, L. Yong Chung, K. Burgess, *Chem. Soc. Rev.* **2013**, *42*, 77-88; c) G. Fan, L. Yang, Z. Chen, *Front. Chem. Sci. Eng.* **2014**, *8*, 405-417; d) A. Díaz-Moscoso, E. Emond, D. L. Hughes, G. J. Tizzard, S. J. Coles, A. N. Cammidge, *J. Org. Chem.* **2014**, *79*, 8932-8934; e) A. Loudet, K. Burgess, in *Handbook of Porphyrin Science Vol. 8* (Eds.: K. M. Kadish, K. M. Smith, R. Guilard), World Scientific, Singapore, **2010**, pp. 1-164.

[4] a) M. Tasior, D. F. O'Shea, *Bioconjugate Chem.* **2010**, *21*, 1130-1133; b) M. Tasior, J. Murtagh, D. O. Frimannsson, S. O. McDonnell, D. F. O'Shea, *Org. Biomol. Chem.* **2010**, *8*, 522-525; c) A. Kamkaew, S. Thavornpradit, T. Puangsamlee, D. Xin, N. Wanichacheva, K. Burgess, *Org. Biomol. Chem.* **2015**, *13*, 8271-8276 ; d) A. Kamkaew, K. Burgess, *Chem. Commun.* **2015**, *51*, 10664-10667

[5] a) J. Killoran, L. Allen, J. F. Gallagher, W. M. Gallagher, D. F. Oshea, *Chem. Commun.* **2002**, 1862-1863; b) N. Adarsh, M. Shanmugasundaram, R. R. Avirah, D. Ramaiah, *Chem. Eur. J.* **2012**, *18*, 12655-12662; c) N. Adarsh, R. R. Avirah, D. Ramaiah, *Org. Lett.* **2010**, *12*, 5720-5723.
[6] a) W.-J. Shi, R. Menting, E. A. Ermilov, P.-C. Lo, B. Roderb, D. K. P. Ng, *Chem. Commun.* **2013**, *49*, 5277-5279; b) F. D'Souza, A. N. Amin, M. E. El-Khouly, N. K. Subbaiyan, M. E. Zandler, S. Fukuzumi, *J. Am. Chem. Soc.* **2011**, *134*, 654-664; c) F. D'Souza, P. M. Smith, M. E. Zandler, A. L. McCarty, M. Itou, Y. Araki, O. Ito, *J. Am. Chem. Soc.* **2004**, *126*, 7898-7907; d) V. Bandi, K. Ohkubo, S. Fukuzumi, F. D'Souza, *Chem. Commun.* **2013**, *49*, 2867-2869; e) V. Bandi, H. B. Gobeze, P. A. Karr, F. D'Souza, *J. Phys. Chem. C* **2014**, *118*, 18969−18982.
[7] P.-A. Bouit, K. Kamada, F. P., G. Berginc, L. Toupet, O. Maury, C. Andraud, *Adv. Mater.* **2009**, *21*, 1151-1154.
[8] M. E. El-Khouly, S. Fukuzumi, F. D'Souza, *ChemPhysChem* **2014**, *15*, 30-47.
[9] a) N. Miyaura, K. Yamada, A. Suzuki, *Tetrahedron Lett.* **1979**, *20*, 3437-3440; b) N. Miyaura, A. Suzuki, *J. Chem. Soc., Chem. Commun.* **1979**, 866-867.
[10] Q. Bellier, S. Pégaz, C. Aronica, B. Le Guennic, C. Andraud, O. Maury, *Org. Lett.* **2010**, *13*, 22-25.
[11] a) A. B. Nepomnyashchii, M. Bröring, J. Ahrens, A. J. Bard, *J. Am. Chem. Soc.* **2011**, *133*, 8633-8643; b) A. B. Nepomnyashchii, A. J. Bard, *Acc. Chem. Res.* **2012**, *45*, 1844-1853.
[12] J. Killoran, L. Allen, J. F. Gallagher, W. M. Gallagher, D. F. Oshea, *Chem. Commun.* **2002**, 1862-1863.
[13] D. Rehm, A. Weller, *Isr. J. Chem.* **1970**, *8*, 259-271.
[14] B. Habermeyer, A. Takai, C. P. Gros, M. El Ojaimi, J.-M. Barbe, S. Fukuzumi, *Chem. Eur.J.* **2011**, *17*, 10670-10681.
[15] H. Lim, S. Seo, S. Pascal, Q. Bellier, S. Rigaut, C. Park, H. Shin, O. Maury, C. Andraud, E. Kim, Sci. Rep. **2015**, *6*, 18867